


## Interaction Control and Bright Solitons in Coherently Coupled Bose-Einstein Condensates

J. Sanz<sup>ⓧ,\*</sup>, A. Frölian<sup>ⓧ</sup>, C. S. Chisholm<sup>ⓧ</sup>, C. R. Cabrera<sup>ⓧ,†</sup> and L. Tarruell<sup>ⓧ,‡</sup>

*ICFO—Institut de Ciències Fotoniques, The Barcelona Institute of Science and Technology, 08860 Castelldefels (Barcelona), Spain*

 (Received 12 December 2019; revised 27 June 2021; accepted 15 November 2021; published 4 January 2022)

We demonstrate fast control of the interatomic interactions in a Bose-Einstein condensate by coherently coupling two atomic states with intra- and interstate scattering lengths of opposite signs. We measure the elastic and inelastic scattering properties of the system and find good agreement with a theoretical model describing the interactions between dressed states. In the attractive regime, we observe the formation of bright solitons formed by dressed-state atoms. Finally, we study the response of the system to an interaction quench from repulsive to attractive values, and observe how the resulting modulational instability develops into a bright soliton train.

DOI: [10.1103/PhysRevLett.128.013201](https://doi.org/10.1103/PhysRevLett.128.013201)

The tunability of interatomic interactions plays a central role in the study of many-body physics with ultracold quantum gases [1]. While interaction control in such systems is traditionally obtained using magnetic Feshbach resonances [2], several of the new frontiers in the field would greatly benefit from a faster control of the scattering length not accessible with this method. Prime examples are the study of out-of-equilibrium dynamics at large energy scales [3], the exploration of driven nonlinear systems [4–6], or the simulation of effective lattice Hamiltonians *via* fast modulations of the interaction strength, for which anyonic excitations and unconventional phases have been predicted [7–9]. In principle, optical Feshbach resonances [10,11] or the manipulation of magnetic Feshbach resonances with optical fields [12–14] fulfill this goal. In practice, these approaches are often plagued by photon-induced atom losses that limit their range of applicability to a handful of atomic species and laser configurations. Therefore, developing new pathways for fast interaction control in quantum gases is highly desirable.

In this Letter, we demonstrate an alternative method for controlling interactions in Bose-Einstein condensates (BECs) which is fast, flexible, and simple to implement experimentally. In our scheme, two internal states with different scattering lengths are coherently coupled exploiting a radio-frequency (rf) field, which modifies the scattering properties of the corresponding dressed states. Until now, this effect could only be observed indirectly through the change of miscibility in binary BEC mixtures [15–17], in a configuration where interactions were modified in a narrow range. Here we show that exploiting a system with inter- and intrastate interactions of opposite signs enables instead large modifications of the elastic and inelastic scattering properties of these dressed states. They can be flexibly controlled by adjusting the parameters of the coupling field, also extending to the attractive regime. In this case, we demonstrate the stabilization of bright solitons

formed by dressed-state atoms. Furthermore, we exploit the high temporal bandwidth of this technique to quench the interactions from repulsive to attractive values, and observe how the resulting modulational instability develops into a bright soliton train.

We perform all experiments in the strong coupling limit, where the Rabi frequency of the rf field  $\Omega$  dominates over all other energy scales of the system. We conveniently describe it using the dressed states  $|-\rangle = \sin\theta|\downarrow\rangle - \cos\theta|\uparrow\rangle$  and  $|+\rangle = \cos\theta|\downarrow\rangle + \sin\theta|\uparrow\rangle$ , which we call the lower and higher dressed state, respectively. The mixing angle  $\theta$  fixes their composition in terms of the bare states  $|\uparrow\rangle$  and  $|\downarrow\rangle$ . It is given by  $\cos^2\theta = (1 + P)/2$ , where  $P = \delta/\tilde{\Omega} = (N_\uparrow - N_\downarrow)/(N_\uparrow + N_\downarrow)$  is the polarization parameter,  $N_\uparrow$  and  $N_\downarrow$  are the bare state populations,  $\delta$  is the detuning of the coupling field, and  $\hbar\tilde{\Omega} = \hbar\sqrt{\Omega^2 + \delta^2}$  is the energy gap between the two dressed states, see Fig. 1(a). Here,  $\hbar$  is the reduced Planck constant.

To describe the interactions between dressed states, we rewrite the interaction part of the Hamiltonian in the dressed-state basis [18]. The resulting collisional couplings account for processes which either preserve the two-particle dressed state of the colliding atoms (elastic processes), or modify it (inelastic processes). For a BEC in state  $|-\rangle$ , inelastic collisions are energetically forbidden and only elastic processes remain. As shown in Fig. 1(b), they can be described through an effective scattering length  $a_{--}$  which depends on the scattering properties of the bare states and on the composition of the system [18,19]. In contrast, for a BEC in state  $|+\rangle$  both elastic and inelastic processes are relevant.

We implement these concepts with a  $^{39}\text{K}$  BEC at magnetic fields  $B \sim 56\text{--}57$  G. We exploit two magnetic sublevels of the  $F = 1$  hyperfine manifold  $|\uparrow\rangle \equiv |F, m_F\rangle = |1, -1\rangle$  and  $|\downarrow\rangle \equiv |1, 0\rangle$ , for which the intrastate scattering lengths are

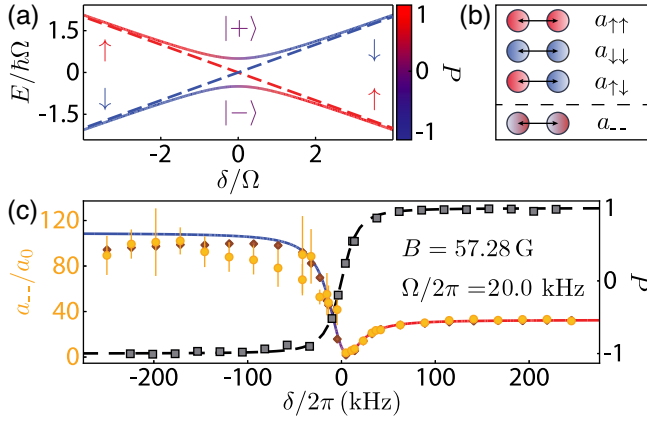


FIG. 1. Elastic scattering properties of the lower dressed state. (a) Energy  $E$  of states  $|-\rangle$  and  $|+\rangle$  vs detuning  $\delta$ , normalized to the Rabi frequency  $\Omega$ .  $\uparrow$  and  $\downarrow$  are the bare atomic states. Color scale: state composition in terms of  $P = \delta/\sqrt{\Omega^2 + \delta^2}$ . (b) Sketch of the bare scattering lengths and resulting effective scattering length  $a_{--}$ . (c) Experimental value of  $a_{--}$  obtained by scaling  $\sigma_x^5/N$  (orange circles, left axis) and  $P$  (gray squares, right axis) vs  $\delta$ . Lines: theory predictions. Brown diamonds: numerical simulation. Color scale of the  $a_{--}$  curve: value of  $P$ . Error bars: standard deviation from 5 independent measurements.

repulsive ( $a_{\uparrow\uparrow}, a_{\downarrow\downarrow} > 0$ ), and the interstate scattering length is attractive ( $a_{\uparrow\downarrow} < 0$ ) [20,21]. We coherently couple the two states with an rf field, with  $\Omega/2\pi > 8$  kHz. We prepare single dressed states through Landau-Zener sweeps, starting from state  $|\uparrow\rangle$  and ramping the detuning  $\delta$  at a rate  $\leq 1$  kHz/ $\mu$ s to its final value [22].

In a first series of experiments we focus on the elastic scattering properties of the lower dressed state  $|-\rangle$ . They are characterized by the effective scattering length  $a_{--} = a_{\uparrow\uparrow}\cos^4\theta + a_{\downarrow\downarrow}\sin^4\theta + \frac{1}{2}a_{\uparrow\downarrow}\sin^2 2\theta$ , and thus depend on the state composition of the system *via*  $\delta$  [18,22].

We experimentally probe this dependency by performing expansion measurements in an optical waveguide. To this end, we prepare a BEC in state  $|-\rangle$  with  $\Omega/2\pi = 20.0(6)$  kHz and variable detuning  $\delta$  using a ramp rate of 0.83 kHz/ms. The magnetic field is set to  $B = 57.280(2)$  G, for which  $a_{\uparrow\uparrow}/a_0 = 32.5$ ,  $a_{\downarrow\downarrow}/a_0 = 109$ ,  $a_{\uparrow\downarrow}/a_0 = -52.9$ , and we always have  $a_{--} > 0$ . Here,  $a_0$  is the Bohr radius. After holding the gas for 5 ms at the final detuning, we abruptly switch off the axial confinement, allowing it to expand for 21 ms along a single-beam optical dipole trap [radial frequency  $\omega_r/2\pi = 133(1)$  Hz]. We finally image the gas *in situ* using a polarization phase contrast scheme [20,21] and exploit the axial size of the cloud  $\sigma_x$  after expansion to infer the scattering length  $a_{--}$  [22]. In the Thomas-Fermi regime the two are related by  $a_{--} \propto \sigma_x^5/N$  [28]. Although this approximation is not strictly valid for all of our experimental parameters, we have verified solving numerically the time-dependent Gross-Pitaevskii equation (GPE) that estimating  $a_{--}$  through

this scaling law results in errors below our experimental uncertainties.

Figure 1(c) shows our determination of  $a_{--}$  for various detunings (circles), corresponding to different values of the polarization parameter  $P$  (squares). We determine it by Stern-Gerlach separation of the bare states during time-of-flight expansion, from which we extract their populations. In order to correct for systematic errors in the measurement and compare the results to the scattering length  $a_{--}$ , we have scaled  $\sigma_x^5/N$  to yield  $a_{\uparrow\uparrow}$  at large positive  $\delta$ . Whereas for large positive (negative) values of  $\delta$  the effective scattering length should approach  $a_{\uparrow\uparrow}$  ( $a_{\downarrow\downarrow}$ ), we expect a minimum at  $\delta/2\pi = 6.5$  kHz ( $P = 0.31$ ) due to the attractive character of the interstate interactions  $a_{\uparrow\downarrow} < 0$ . This is in good agreement with the experimental measurements. The data at large negative  $\delta$  are in fair agreement with the limit  $a_{\downarrow\downarrow}$ . It is in this regime that the scaling law yields the largest discrepancies with the GPE simulations (diamonds) [29]. In conclusion, this method provides tunability of  $a_{--}$  by more than  $100a_0$  without introducing additional loss mechanisms [22].

Next, we consider the scattering properties of the higher dressed state  $|+\rangle$ . There, besides elastic collisions, two-body inelastic collisions leading to a change of the two-particle dressed state are also allowed. For our typical experimental parameters they limit the lifetime of the BEC to  $\sim 1$  ms. Figure 2(a) sketches the two possible inelastic processes: ①  $|++\rangle \rightarrow |--\rangle$  and ②  $|++\rangle \rightarrow (|+-\rangle + |-+\rangle)/\sqrt{2}$ . Both lead to the creation of correlated atom pairs with opposite momenta. They are accompanied by an energy release of either  $\hbar\Omega$  or  $\hbar\Omega/2$  per atom, corresponding to the energy gap between the two-particle dressed states. Similar processes occur in Raman-coupled BECs [30].

To reveal these dressed-state changing collisions, we rapidly prepare (ramp rate 500 kHz/ms) a pure sample of  $|+\rangle$  atoms. We then immediately switch off the trap and let the gas expand for a time  $t_{\text{exp}}$ . During the first 1 ms the rf field is kept on, allowing us to characterize the decay processes in the absence of the trap. As depicted in Fig. 2(b), the time-of-flight images reveal the presence of halos of atoms expanding away from the condensate [22]. Since atoms in a BEC scatter with extremely low relative momenta, the halo radius  $R_H$  at time  $t_{\text{exp}}$  directly reflects the velocity of the collision products  $v_f = R_H/t_{\text{exp}}$ . Processes ① and ② can be distinguished because the velocities are given by  $v_1 = \sqrt{2\hbar\Omega/m}$  and  $v_2 = \sqrt{\hbar\Omega/m}$ , respectively, where  $m$  is the mass of  $^{39}\text{K}$ . In these expressions, we have neglected the released mean-field energy of the BEC since the corresponding correction remains well below our experimental resolution. Interestingly, we observe that the likelihood of the two processes depends on the dressed state composition, and thus on  $\delta$ .

Figures 2(c), 2(d), and 2(e) present a more systematic study of these inelastic processes as a function of the

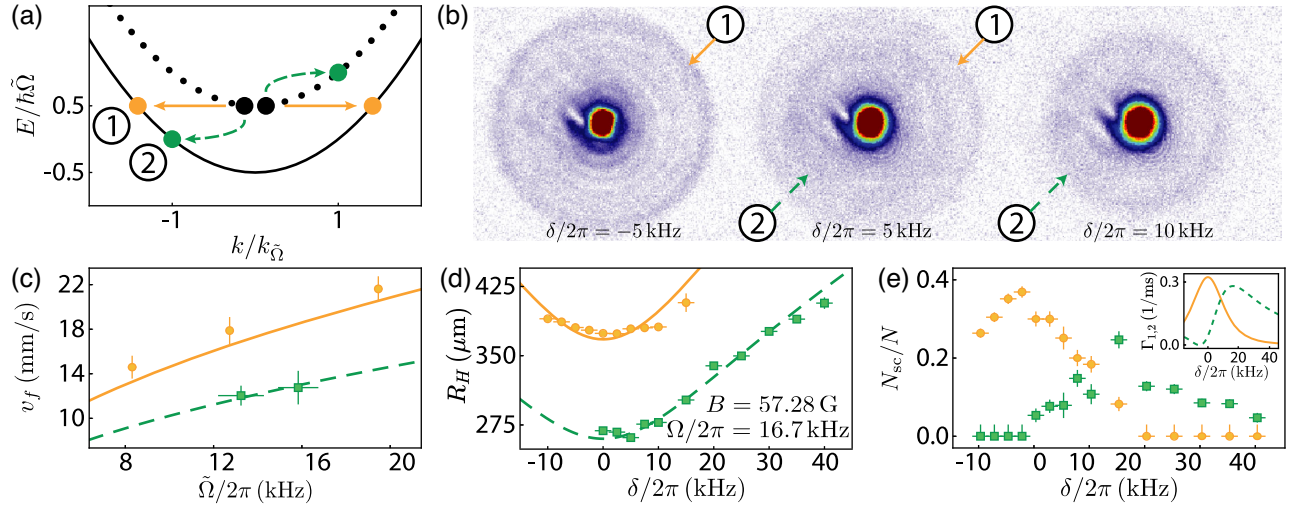


FIG. 2. Inelastic decay of the higher dressed state. (a) Sketch of possible dressed state changing collisions ①:  $|++\rangle \rightarrow |--\rangle$  (orange, solid arrows) and ②:  $|++\rangle \rightarrow (|+-\rangle + |-+\rangle)/\sqrt{2}$  (green, dashed arrows). Energy  $E$  and momentum  $k$  are normalized by  $\tilde{\Omega} = \sqrt{\Omega^2 + \delta^2}$  and  $k_{\tilde{\Omega}} = \sqrt{m\tilde{\Omega}}/\hbar$ . (b) Momentum distribution of the collision products. Images are the average of 10 independent measurements. The likelihood of processes ① and ② depends on  $\delta$ . (c) Velocity of the scattered atoms  $v_f$  vs  $\tilde{\Omega}$ . (d) Radius of the halos  $R_H$  for an expansion time  $t_{\text{exp}} = 20.1$  ms. (e) Fraction of scattered atoms  $N_{sc}/N$  vs  $\delta$ . Inset: Inelastic scattering rate  $\Gamma_{1,2}$  vs  $\delta$  for  $n = 1.3 \times 10^{14}$  atoms/cm<sup>3</sup>. In (c), (d), and (e) orange circles (green squares) correspond to process ① (②). Lines: noninteracting theory. Error bars: fit error (vertical) and uncertainty of  $\delta$  and  $\tilde{\Omega}$  (horizontal).

parameters of the coupling field. Figure 2(c) depicts the velocity of the atoms in each halo vs  $\tilde{\Omega}$ , determined by measuring  $R_H$  for different values of  $t_{\text{exp}}$  [22]. Figure 2(d) shows the measured halo radius as a function of  $\delta$ , with circles (squares) corresponding to process ① (②). The measurements are in excellent agreement with the theory predictions neglecting the BEC mean-field energy without any fitting parameters (solid and dashed lines).

The scattering cross section of the two processes strongly depends on detuning. This can be clearly seen in Fig. 2(e), where we plot the fraction of atoms scattered in each halo  $N_{sc}/N$  as a function of  $\delta$  extracted from the same set of images as Fig. 2(d). The rate equation describing the evolution of the density in the initial state reads  $\dot{n} = -2(\Gamma_1 + \Gamma_2)n = -2g^{(2)}(\sigma_1 v_1 + \sigma_2 v_2)(n^2/2)$ . Here  $\Gamma_{1,2}$  are the inelastic scattering rates for processes ① and ②,  $g^{(2)} = 1$  is the BEC two-body correlation function,  $n^2/2$  is the density of atom pairs, and  $\sigma_1 = \pi[(a_{\uparrow\uparrow} + a_{\downarrow\downarrow} - 2a_{\uparrow\downarrow})\sin^2 2\theta]^2/2$  and  $\sigma_2 = 4\pi[(a_{\uparrow\uparrow}\sin^2\theta - a_{\downarrow\downarrow}\cos^2\theta + a_{\uparrow\downarrow}\cos 2\theta)\sin 2\theta]^2$  are the corresponding scattering cross sections [18,22]. Our measurements agree qualitatively with the expected  $\Gamma_{1,2}$  line shapes, see inset. For a quantitative prediction, the simultaneous reduction of  $n$  due to the 1 ms expansion of the cloud (which depends on  $\delta$  via  $a_{++}$ ) must be taken into account. For  $\delta \sim 0$ , the expansion can be neglected and  $\sigma_2 \sim 0$ , greatly simplifying the dynamics. In this regime, integration of the rate equation yields  $N_{sc}/N \sim 0.28$  for an initial density  $n \sim 1.3 \times 10^{14}$  atoms/cm<sup>3</sup>, in good agreement with the experiment.

After demonstration of the different collisional couplings present in dressed BECs, we refocus on the lower dressed state  $|-\rangle$  and exploit the broad tunability of its effective scattering length to explore attractively interacting systems. In optical waveguides, this situation enables the study of bright solitons: matter-wave packets that propagate without changing their shape because attractive non-linearities balance the effect of dispersion along the unconfined direction [31,32]. In coherently coupled systems, they are formed by dressed atoms constituting dressed-state bright solitons. Compared to conventional solitons, they are bound by an additional mean-field attractive nonlinearity that scales with density as an effective three-body force [22]. They are only stable while the gas is effectively one dimensional, with an interaction energy that remains below  $\hbar\omega_r$  [33–35].

To observe this new type of bright soliton, we study the dynamics of a BEC in state  $|-\rangle$  after release in an optical waveguide. The magnetic field is set to  $B = 56.000(2)$  G, where  $a_{\uparrow\uparrow}/a_0 = 35.1$ ,  $a_{\downarrow\downarrow}/a_0 = 57.9$ ,  $a_{\uparrow\downarrow}/a_0 = -53.5$ , and  $a_{--}$  can take negative values, see Fig. 3(a). We adiabatically prepare the system at different detunings (ramp rate 1 kHz/ms). For  $a_{--} < 0$  we keep the initial atom number below  $N \sim 3000$  to avoid collapse [22]. We then remove the axial confinement in 15 ms, allowing for free evolution in the waveguide. Figure 3(b) shows *in situ* images after an evolution time  $t_g$ . For  $\delta/2\pi = \pm 250$  kHz the gas expands, as expected for a repulsive BEC in states  $|\uparrow\rangle$  or  $|\downarrow\rangle$ , whereas for  $\delta = 0$  its shape remains unchanged. Here  $a_{--}/a_0 = -3.5$  and we observe the formation of a single dressed-state bright soliton.

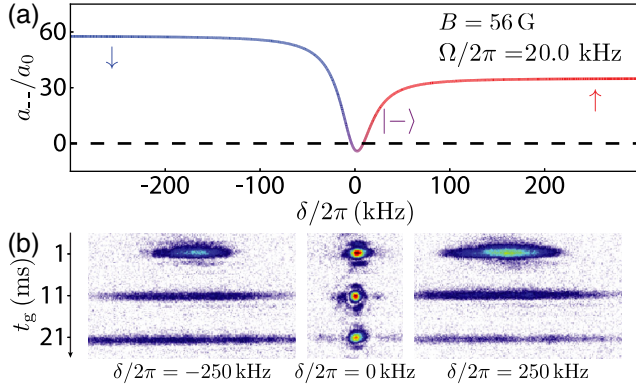


FIG. 3. Formation of a dressed-state bright soliton. (a)  $a_{-}$  vs  $\delta$ . Near zero detuning  $a_{-} < 0$ . (b) *In situ* dynamics of the gas after an evolution time  $t_g$  in the optical waveguide. For  $\delta/2\pi = 0$  ( $a_{-}/a_0 = -3.5$ ) a self-bound bright soliton forms. For  $\delta/2\pi = 250$  kHz [ $N = 9(2) \times 10^4$ ] and  $\delta/2\pi = -250$  kHz [ $N = 1.0(2) \times 10^4$ ],  $a_{-} > 0$  and the gas expands.

In the last series of experiments, we explore the response of the system to a quench of the effective scattering length from repulsive to attractive values. As demonstrated in recent experiments [36,37], this triggers a modulational instability in the BEC: a mechanical instability where fluctuations in the condensate density are exponentially enhanced by the attractive nonlinearity. Consequently, the gas splits into several components. The growth of the density modulation is dominated by the most unstable Bogoliubov modes, which have characteristic momentum  $k_{\text{MI}} \sim 1/\xi$ . Here,  $\xi = a_{\text{ho}}/\sqrt{4|a_{-}|n_{1\text{D}}}$  is the healing length of the BEC in the waveguide,  $a_{\text{ho}} = \sqrt{\hbar/m\omega_r}$  is the radial harmonic oscillator length, and  $n_{1\text{D}}$  is the line density of the system before the quench. The characteristic length and time scales of this process are  $\lambda = 2\pi/k_{\text{MI}}$  and  $\tau_{\text{MI}} = 2m/\hbar k_{\text{MI}}^2$ , respectively. For  $t > \tau_{\text{MI}}$ , each of the components evolves into a bright soliton, forming a soliton train [31,38–41]. For a system of size  $L$  at the moment of the quench, the average number of solitons is expected to be  $N_S = L/\lambda$ , from length scale arguments [39]. This prediction has been verified experimentally only in a restricted range of scattering lengths due to limitations in the quench timescales [36,37].

Our experimental sequence is summarized in Fig. 4(a). The starting point is a BEC of  $65(15) \times 10^3$  atoms confined in a crossed trap [22]. At  $t = 0$  we switch off the axial confinement and let the atoms expand in the waveguide for  $t_g = 11$  ms, reaching a size  $L \sim 112 \mu\text{m}$ . At this point, we abruptly change  $\delta$  (ramp rate 1 kHz/ $\mu\text{s}$ ), effectively quenching the scattering length from  $35.1a_0$  to its final value. An additional expansion time of 10 ms allows the development of the modulational instability and the formation of a soliton train, which we image *in situ*.

Figure 4(b) shows the average number of components observed per image  $N_S$  as a function of the final detuning

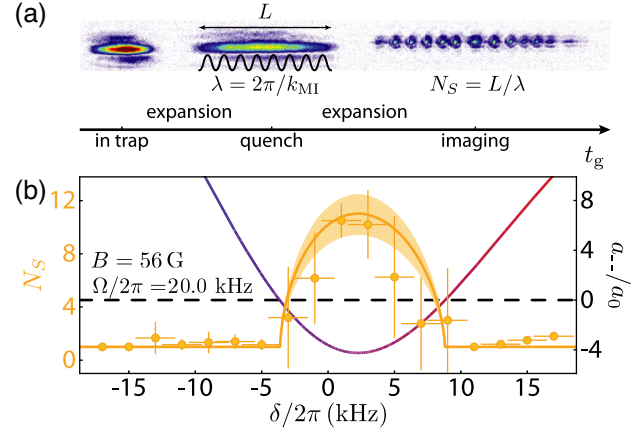


FIG. 4. Modulational instability and formation of bright soliton trains. (a) Sketch of the experimental sequence and exemplary *in situ* images. (b) Number of components observed per image  $N_S$  vs  $\delta$  after the quench (orange circles). Error bars: standard deviation of 4 to 6 independent measurements (vertical) and uncertainty of  $\delta$  (horizontal). Orange line, left axis: theory prediction  $N_S = L/\lambda$  (shaded area: uncertainty due to the systematic error in the atom number). Colored line, right axis:  $a_{-}$  (color scale: value of  $P$ ).

[22]. While the initial BEC has  $N_S = 1$ , for all values of  $\delta$  such that  $a_{-} < 0$  we measure  $N_S > 1$ . The maximum number of solitons in a train is observed at  $\delta/2\pi = 2.3$  kHz, which corresponds to the most attractive value of  $a_{-}/a_0 = -4.2$ . This value is 2.5 times more negative than in previous experiments, where interactions were controlled using magnetic Feshbach resonances [36,37]. Indeed, our dressed-state approach enables ramp rates orders of magnitude faster, ensuring a clear separation of timescales vs  $\tau_{\text{MI}}$  and making three-body recombination processes during the quench negligible. As a result, we are able to verify the validity of the scaling prediction  $N_S = L/\lambda$  in a much broader range of parameters [22].

In conclusion, we have demonstrated fast and flexible control of the collisional properties in rf-coupled  $^{39}\text{K}$  BECs. In the attractive regime, we have observed the formation of dressed-state bright solitons, and studied how the modulational instability triggered by an interaction quench develops into a soliton train. Our work opens exciting perspectives. First, dressed-state changing collisions could be exploited as a tunable source of correlated atom pairs for atom optics experiments, complementary to other approaches [42–46]. Second, rf-coupled BECs with attractive interactions are expected to display novel types of nonlinearities stemming from beyond mean-field effects. In the weak coupling limit, they scale as three-body forces and should stabilize new types of quantum droplets [47,48]. Finally, control of interactions by coherent coupling *via* optical Raman transitions provides spatial control of the effective scattering length, and constitutes an ideal platform for implementing density-dependent gauge fields and realizing chiral solitons [49].

We thank J. Brand, D. S. Petrov, A. Recati, and L. Santos for insightful discussions, A. Simoni for providing the scattering lengths of Ref. [50] in numerical form, and A. Celi, E. Neri, and R. Ramos for a careful reading of the manuscript. We acknowledge funding from Fundació Privada Cellex, Fundació Mir-Puig, European Union (ERC CoG SuperComp–101003295), Ministerio de Ciencia e Innovación and Agencia Estatal de Investigación/10.13039/501100011033 (QuDROP FIS2017-88334-P, LIGAS PID2020-112687GB-C21, and Severo Ochoa No. CEX2019-000910-S), Deutsche Forschungsgemeinschaft (Research Unit FOR2414, Project No. 277974659), Fundación Ramón Areces (CODEC), European Union Regional Development Fund within the ERDF Operational Program of Catalunya (project QUASICAT/QuantumCat Ref. No. 001-P-001644), and Generalitat de Catalunya (SGR1660 and CERCA program). J. S. acknowledges support from Ministerio de Ciencia e Innovación (BES-2015-072186), A.F. from La Caixa Foundation (ID 100010434, PhD fellowship LCF/BQ/DI18/11660040) and the European Union (Marie Skłodowska-Curie–713673), C. S. C. from the European Union (Marie Skłodowska-Curie–713729), C. R. C. from an ICFO-MPQ Cellex postdoctoral fellowship, and L. T. from Ministerio de Ciencia e Innovación/Agencia Estatal de Investigación/10.13039/501100011033, and European Social Fund “Investing in your future” (RYC-2015-17890/10.13039/501100011033).

*Note added in the proof.*—While this work was under review, evidence for some of the beyond mean-field effects discussed in the outlook have been observed by the Institut d’Optique group [48].

\*Present address: Quside Technologies S.L., C/ Esteve Terradas 1, 08860 Castelldefels (Barcelona), Spain.

†Present address: Fakultät für Physik, Ludwig-Maximilians-Universität, Schellingstr. 4, D-80799 München, Germany, and Max-Planck-Institut für Quantenoptik, Hans-Kopfermann-Strasse 1, D-85748 Garching, Germany.

‡leticia.tarruell@icfo.eu

- [1] I. Bloch, J. Dalibard, and W. Zwerger, Many-body physics with ultracold gases, *Rev. Mod. Phys.* **80**, 885 (2008).
- [2] C. Chin, R. Grimm, P. Julienne, and E. Tiesinga, Feshbach resonances in ultracold gases, *Rev. Mod. Phys.* **82**, 1225 (2010).
- [3] A. Bulgac and S. Yoon, Large Amplitude Dynamics of the Pairing Correlations in a Unitary Fermi Gas, *Phys. Rev. Lett.* **102**, 085302 (2009).
- [4] K. Staliunas, S. Longhi, and G. J. de Valcárcel, Faraday Patterns in Bose-Einstein Condensates, *Phys. Rev. Lett.* **89**, 210406 (2002).
- [5] F. Kh. Abdullaev, J. G. Caputo, R. A. Kraenkel, and B. A. Malomed, Controlling collapse in Bose-Einstein condensates by temporal modulation of the scattering length, *Phys. Rev. A* **67**, 013605 (2003).
- [6] H. Saito and M. Ueda, Bose-Einstein droplet in free space, *Phys. Rev. A* **70**, 053610 (2004).
- [7] J. Gong, L. Morales-Molina, and P. Hänggi, Many-body Coherent Destruction of Tunneling, *Phys. Rev. Lett.* **103**, 133002 (2009).
- [8] S. Greschner, G. Sun, D. Poletti, and L. Santos, Density-Dependent Synthetic Gauge Fields Using Periodically Modulated Interactions, *Phys. Rev. Lett.* **113**, 215303 (2014).
- [9] S. Greschner, L. Santos, and D. Poletti, Exploring Unconventional Hubbard Models with Doubly Modulated Lattice Gases, *Phys. Rev. Lett.* **113**, 183002 (2014).
- [10] M. Theis, G. Thalhammer, K. Winkler, M. Hellwig, G. Ruff, R. Grimm, and J. H. Denschlag, Tuning the Scattering Length with an Optically Induced Feshbach Resonance, *Phys. Rev. Lett.* **93**, 123001 (2004).
- [11] K. Enomoto, K. Kasa, M. Kitagawa, and Y. Takahashi, Optical Feshbach Resonance Using the Intercombination Transition, *Phys. Rev. Lett.* **101**, 203201 (2008).
- [12] D. M. Bauer, M. Lettner, C. Vo, G. Rempe, and S. Dürr, Control of a magnetic Feshbach resonance with laser light, *Nat. Phys.* **5**, 339 (2009).
- [13] L. W. Clark, L.-C. Ha, C.-Y. Xu, and C. Chin, Quantum Dynamics with Spatiotemporal Control of Interactions in a Stable Bose-Einstein Condensate, *Phys. Rev. Lett.* **115**, 155301 (2015).
- [14] A. Jagannathan, N. Arunkumar, J. A. Joseph, and J. E. Thomas, Optical Control of Magnetic Feshbach Resonances by Closed-Channel Electromagnetically Induced Transparency, *Phys. Rev. Lett.* **116**, 075301 (2016).
- [15] E. Nicklas, H. Strobel, T. Zibold, C. Gross, B. A. Malomed, P. G. Kevrekidis, and M. K. Oberthaler, Rabi Flopping Induces Spatial Demixing Dynamics, *Phys. Rev. Lett.* **107**, 193001 (2011).
- [16] E. Nicklas, M. Karl, M. Höfer, A. Johnson, W. Muessel, H. Strobel, J. Tomković, T. Gasenzer, and M. K. Oberthaler, Observation of Scaling in the Dynamics of a Strongly Quenched Quantum Gas, *Phys. Rev. Lett.* **115**, 245301 (2015).
- [17] K. Shibata, A. Torii, H. Shibayama, Y. Eto, H. Saito, and T. Hirano, Interaction modulation in a long-lived Bose-Einstein condensate by rf coupling, *Phys. Rev. A* **99**, 013622 (2019).
- [18] C. P. Search and P. R. Berman, Manipulating the speed of sound in a two-component Bose-Einstein condensate, *Phys. Rev. A* **63**, 043612 (2001).
- [19] D. S. Petrov, Three-Body Interacting Bosons in Free Space, *Phys. Rev. Lett.* **112**, 103201 (2014).
- [20] C. R. Cabrera, L. Tanzi, J. Sanz, B. Naylor, P. Thomas, P. Cheiney, and L. Tarruell, Quantum liquid droplets in a mixture of Bose-Einstein condensates, *Science* **359**, 301 (2018).
- [21] P. Cheiney, C. R. Cabrera, J. Sanz, B. Naylor, L. Tanzi, and L. Tarruell, Bright Soliton to Quantum Droplet Transition in a Mixture of Bose-Einstein Condensates, *Phys. Rev. Lett.* **120**, 135301 (2018).
- [22] See Supplemental Material at <http://link.aps.org/supplemental/10.1103/PhysRevLett.128.013201>, which includes as well Refs. [23–27], for additional information on the tuning range and rate of change of the effective scattering length, the effect

- of three-body recombination, and the experimental parameters and data analysis.
- [23] Y. Li, L. P. Pitaevskii, and S. Stringari, Quantum Tricriticality and Phase Transitions in Spin-Orbit Coupled Bose-Einstein Condensates, *Phys. Rev. Lett.* **108**, 225301 (2012).
- [24] C. D'Errico, M. Zaccanti, M. Fattori, G. Roati, M. Inguscio, G. Modugno, and A. Simoni, Feshbach resonances in ultracold  $^{39}\text{K}$ , *New J. Phys.* **9**, 223 (2013).
- [25] L. Tanzi, C. R. Cabrera, J. Sanz, P. Cheiney, M. Tomza, and L. Tarruell, Feshbach resonances in potassium Bose-Bose mixtures, *Phys. Rev. A* **98**, 062712 (2018).
- [26] J. Sanz, Two-component Bose-Einstein condensates with competing interactions, Ph.D. thesis, UPC, 2020, <https://www.tdx.cat/handle/10803/668865#page=1>.
- [27] R. A. Williams, M. C. Beeler, L. J. LeBlanc, K. Jiménez-García, and I. B. Spielman, Raman-Induced Interactions in a Single-Component Fermi Gas Near an s-Wave Feshbach Resonance, *Phys. Rev. Lett.* **111**, 095301 (2013).
- [28] Y. Castin and R. Dum, Bose-Einstein Condensates in Time Dependent Traps, *Phys. Rev. Lett.* **77**, 5315 (1996).
- [29] The data has larger uncertainties due to residual breathing excitations induced by the detuning ramp and the large three-body recombination rate of state  $|\downarrow\rangle$  [22].
- [30] R. A. Williams, L. J. LeBlanc, K. Jiménez-García, M. C. Beeler, A. R. Perry, W. D. Phillips, and I. B. Spielman, Synthetic partial waves in ultracold atomic collisions, *Science* **335**, 6066 (2012).
- [31] K. E. Strecker, G. B. Partridge, A. G. Truscott, and R. G. Hulet, Formation and propagation of matter-wave soliton trains, *Nature (London)* **417**, 150 (2002).
- [32] L. Khaykovich, F. Schreck, G. Ferrari, T. Bourdel, J. Cubizolles, L. D. Carr, Y. Castin, and C. Salomon, Formation of a matter-wave bright soliton, *Science* **296**, 1290 (2002).
- [33] V. M. Pérez-García, H. Michinel, and H. Herrero, Bose-Einstein solitons in highly asymmetric traps, *Phys. Rev. A* **57**, 3837 (1998).
- [34] L. Salasnich, A. Parola, and L. Reatto, Condensate bright solitons under transverse confinement, *Phys. Rev. A* **66**, 043603 (2002).
- [35] L. D. Carr and Y. Castin, Dynamics of a matter-wave bright soliton in an expulsive potential, *Phys. Rev. A* **66**, 063602 (2002).
- [36] J. H. V. Nguyen, D. Luo, and R. G. Hulet, Formation of matter-wave soliton trains by modulational instability, *Science* **356**, 422 (2017).
- [37] P. J. Everitt, M. A. Sooriyabandara, M. Guasoni, P. B. Wigley, C. H. Wei, G. D. McDonald, K. S. Hardman, P. Manju, J. D. Close, C. C. N. Kuhn, S. S. Szigeti, Y. S. Kivshar, and N. P. Robins, Observation of a modulational instability in Bose-Einstein condensates, *Phys. Rev. A* **96**, 041601(R) (2017).
- [38] U. Al Khawaja, H. T. C. Stoof, R. G. Hulet, K. E. Strecker, and G. B. Partridge, Bright Soliton Trains of Trapped Bose-Einstein Condensates, *Phys. Rev. Lett.* **89**, 200404 (2002).
- [39] L. Salasnich, A. Parola, and L. Reatto, Modulational Instability and Complex Dynamics of Confined Matter-Wave Solitons, *Phys. Rev. Lett.* **91**, 080405 (2003).
- [40] L. D. Carr and J. Brand, Spontaneous Soliton Formation and Modulational Instability in Bose-Einstein Condensates, *Phys. Rev. Lett.* **92**, 040401 (2004).
- [41] L. D. Carr and J. Brand, Pulsed atomic soliton laser, *Phys. Rev. A* **70**, 033607 (2004).
- [42] M. Greiner, C. A. Regal, J. T. Stewart, and D. S. Jin, Probing Pair-Correlated Fermionic Atoms through Correlations in Atom Shot Noise, *Phys. Rev. Lett.* **94**, 110401 (2005).
- [43] I. B. Spielman, P. R. Johnson, J. H. Huckans, C. D. Fertig, S. L. Rolston, W. D. Phillips, and J. V. Porto, Collisional deexcitation in a quasi-two-dimensional degenerate bosonic gas, *Phys. Rev. A* **73**, 020702(R) (2006).
- [44] A. Perrin, H. Chang, V. Krachmalnicoff, M. Schellekens, D. Boiron, A. Aspect, and C. I. Westbrook, Observation of Atom Pairs in Spontaneous Four-Wave Mixing of Two Colliding Bose-Einstein Condensates, *Phys. Rev. Lett.* **99**, 150405 (2007).
- [45] R. Bücke, J. Grond, S. Manz, T. Berrada, T. Betz, C. Koller, U. Hohenester, T. Schumm, A. Perrin, and J. Schmiedmayer, Twin-atom beams, *Nat. Phys.* **7**, 608 (2011).
- [46] B. Lücke, M. Scherer, J. Kruse, L. Pezz, F. Deuretzbacher, P. Hyllus, O. Topic, J. Peise, W. Ertmer, J. Arlt, L. Santos, A. Smerzi, and C. Klempt, Twin matter waves for interferometry beyond the classical limit, *Science* **334**, 773 (2011).
- [47] A. Cappellaro, T. Macrì, G. F. Bertacco, and L. Salasnich, Equation of state and self-bound droplet in Rabi-coupled Bose mixtures, *Sci. Rep.* **7**, 13358 (2017).
- [48] L. Lavoine, A. Hammond, A. Recati, D. S. Petrov, and T. Bourdel, Beyond-Mean-Field Effects in Rabi-Coupled Two-Component Bose-Einstein Condensate, *Phys. Rev. Lett.* **127**, 203402 (2021).
- [49] M. J. Edmonds, M. Valiente, G. Juzeliūnas, L. Santos, and P. Öhberg, Simulating an Interacting Gauge Theory with Ultracold Bose Gases, *Phys. Rev. Lett.* **110**, 085301 (2013).
- [50] S. Roy, M. Landini, A. Trenkwalder, G. Semeghini, G. Spagnolli, A. Simoni, M. Fattori, M. Inguscio, and G. Modugno, Test of the Universality of the Three-Body Efimov Parameter at Narrow Feshbach Resonances, *Phys. Rev. Lett.* **111**, 053202 (2013).